Review paper

Numerical analysis of the influence of mining ground deformation on the structure of a masonry residential building

L. Szojda[1], Ł. Kapusta[2]

Abstract: The article presents numerical analysis of a typical residential building in the Upper Silesian Coal Basin, which was erected in the early twentieth century and was not protected against mining ground deformations. The greatest impact of ground deformation on buildings are ground horizontal strain ε and ground curvature K. Numerical calculations included the building and the ground to take into account the effect of soil-structure interaction. The structure of the analysed building was made of masonry with wooden ceiling and roof elements. The ground was implemented as a layer 3.0m below the foundations and 3.0 m outside the building's projection. Construction loads are divided into two stages – permanent and functional loads as well as ground mining deformation. The maximum convex curvature $K+$ and the horizontal strain of the substrate $\varepsilon+$ were achieved in the 8th load step. The results of the analyses were presented in the form of stress and deformation maps. The most important results are the magnitude of the main tensile stresses σ_{max}, which could to create cracks in the structure may occur after exceeding the tensile strength f_t of the material. The presented method can be used to the analysis of endangered building objects by mining ground deformations.

Keywords: masonry structures, numerical analysis, mining subsidence, ground curvature, ground horizontal strain

[1] Prof., DSc., PhD., Eng., Silesian University of Technology, Department of Structural Engineering, ul. Akademicka 5, 44-100 Gliwice, Poland; e-mail: leszek.szojda@polsl.pl ORCID: https://orcid.org/0000-0002-9919-6263

[2] PhD., Eng., Kielce University of Technology, Department of Environmental, Geomatic and Energy Engineering, al. Tysiąclecia Państwa Polskiego 7, 25-314 Kielce, Poland, e-mail: kapusta.lukasz@gmail.com ORCID: https://orcid.org/0000-0003-4842-135X

1. Introduction

The urban buildings of Upper Silesian Coal Basin (USCB) have developed over the centuries and a large proportion of the current residential buildings date back to the beginning of the 20th century. A significant increase in housing construction dates back to this period and it was connected with the development of heavy industry, particularly mining. Buildings constructed at that time were usually adapted to take over the impact of soil deformations caused by mining. One of the few methods that were used at that time was the division of a structure into smaller segments, which allowed for limiting the increase of internal forces in the event of ground deformations. Nevertheless, the impact of terrain deformation on buildings caused an increase in internal forces that could lead to damage to the building structures.

The problem of structural building damage due to soil deformation, caused by the mining industry, is still relevant. Newly constructed buildings are designed and erected in accordance with the recommendations given in the relevant standards. Existing buildings, however, are often in a worse technical state and not secured against such influences. Determining the size and shape of the soil deformation, and thus the increase of loads and internal forces in the structure, is the most important step in ensuring the safe operation of the building.

This article presents a numerical analysis of an actual building that was erected at the beginning of the previous century, using traditional technology and subjected to the influence of mining ground deformations. The building was subjected to the effects of ground deformations which were caused by the exploitation of the coal bed lying directly below it.

Ground deformations caused by mineral exploitation can be classified as continuous or discontinuous in [1]. Ground deformations are also accompanied by ground tremors, which affect building structures, which was presented e.g. in [2], [3], [4]. Continuous deformation occurred in the majority of cases, as described by various authors such as [5], [6], [7]. A theory for predicting soil deformation due to mining had already been proposed by the beginning of the 20th century. The first theory of subsidence prediction for a mining field of any shape, based on the geometry-integral relation, was proposed in the 1930s [8]. Computational methods began to be intensely developed, particularly in [8], [9], [10] and also [11]. In the largest coal-producing countries (China, the USA and the countries of Central and Eastern Europe, particularly Poland), the theory put forward in [9] was used to calculate the soil deformation; this was also described in [12] and [13]. According to that theory, ground deformation is described by five parameters: settlement w, tilt T, radius of curvature R (or curvature $K = 1/R$), horizontal displacement U and horizontal strain ε. The

theoretical basis for the behaviour of building structures under these influences was given in [14] and, according to its assumptions, the number of significant ground parameters can be reduced to two: curvature K and horizontal strain ε.

2. Background

Determining the actual values of the direct impact on a structure is no longer unambiguous and depends on many factors. When analysing the structure affected by soil deformation, it is necessary to take into account the rigidity of the structure and soil properties at the foundation level. Detailed analysis of a building's structural response to ground deformation should be considered as a set soil-structure interaction. The complex relations between a building and the terrain are best resolved by advanced numerical analysis, which should be verified for the actual construction. Attempts at the numerical analyses of these types of problems are rare. The issues regarding the influence of terrain curvature on buildings are presented in [15] and [16]. They described a structure's vulnerability according to the materials used and building geometry, depending on the predicted mining subsidence. Protection of the building against the influence of soil deformation is in this case a natural engineering operation. Typical solutions of such treatments, with respect to buildings, are shown in [17], [18], [19] and [20]. The protection of buildings through geotechnical solutions are less developed but were presented in [21] and [22]. Some similar considerations regarding the construction of buildings have been presented [23], [24], [25].

Because the operating period of the coalbed exploitation was known and the surrounding area (as well as the objects themselves) was measured, the measured points were stabilised in the ground directly at the building location and on the longitudinal walls above ground level. In this case, the location of the structures subjected to measurements was such that the direction of the revealed deformations was parallel to the longer axes of the buildings. The measurements were being carried out as the deformations were revealed, which allowed for determining horizontal deformations in the ground and the curvature of the terrain, as well as the curvature of the building structures. The adequate accuracy was achieved by using of method of precision levelling. Fig. 1 shows the location of the measuring points on one of the buildings and the adjacent measuring line. An assessment of the extent of the damage to the structures was made before and after the appearance of all the influences. This became the basis for confirming the validity of the results of the numerical analysis.
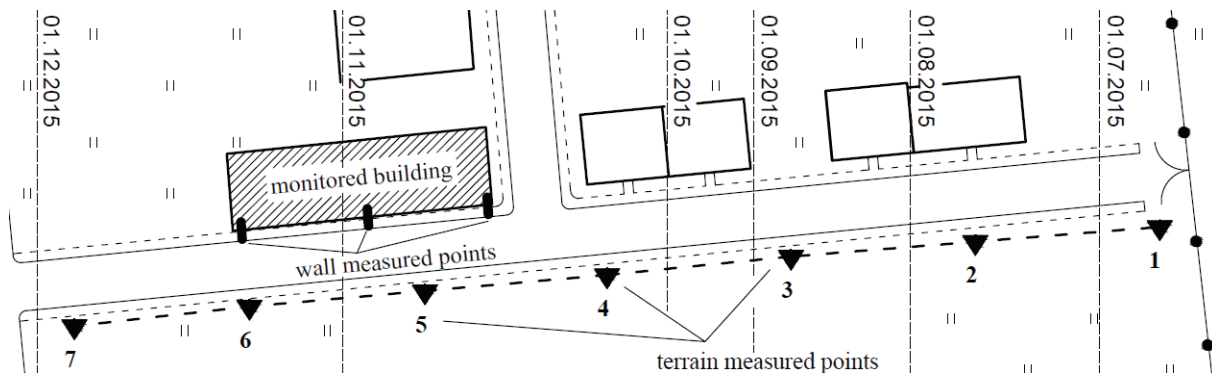
Fig. 1. Location of measured points and progress of the mining longwall operational front under the monitored area

3. Soil-structure interaction layout assumed for the numerical analysis

3.1. Building structure and ground parameters

The building that was the subject of this study, which was subjected to mining-induced ground deformation, consisted of one segment and had projection dimensions of 44.3×11.8 m. The structure of the building was typical for the USCB region: masonry with a wooden structure forming the above-ground floor and roof. Depending on the position, the thickness of the basement walls were 52 cm and the walls above were 38 cm thick. The masonry material was assumed to be homogeneous. The material parameters adopted for the analyses were determined based on macroscopic studies and adopted on the basis of [19]:

- compressive strength of the wall $f_k = 2.2$ MPa,
- volumetric weight of the wall $\gamma = 18$ kN/m^3,
- long-lasting modulus of elasticity of the wall $E = 900$ MPa.

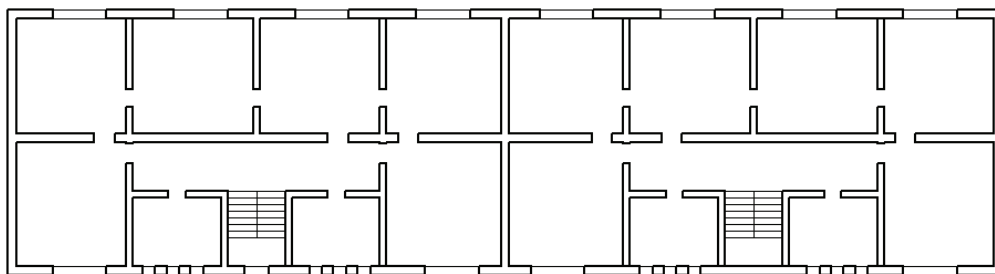A schematic projection of typical floor is shown in Fig. 2.

Fig. 2. Schematic projection of the typical floor for the monitored building

The analysis does not take into account wooden ceilings or roof constructions due to their insignificant stiffness; they do not constitute stiffeners for the bent building.

After making the outcrop in the foundation level, clay was found to be in a hard-plastic state with the following parameters:

- degree of plasticity $I_L = 0.2$,
- internal friction angle $\varphi = 18°$,
- cohesion $c = 32$ kPa.

3.2. Mining-inducted ground deformation

The excavated longwall panel was located below the observed building. The longwall front moved in a direction that was longitudinal to the long wall of the building. The basic parameters of the excavated coal seam (located directly under the building) were as follows:

- average depth of the exploited seam of coal   710 m,
- longwall panel length   1900 m,
- longwall panel width   400 m,
- thickness of the exploited longwall panel   1.8 m,
- method of deposit exploitation   caving carried out,
- time of exploitation of longwall panel   August 2014 – March 2016.

Deformations of the ground and building were observed on embedded measured points (Fig. 1). The observations were made during the whole period, revealing influences and being repeated weekly. The most interesting results, with respect to the subsiding ground measured points, are presented in Fig. 3.
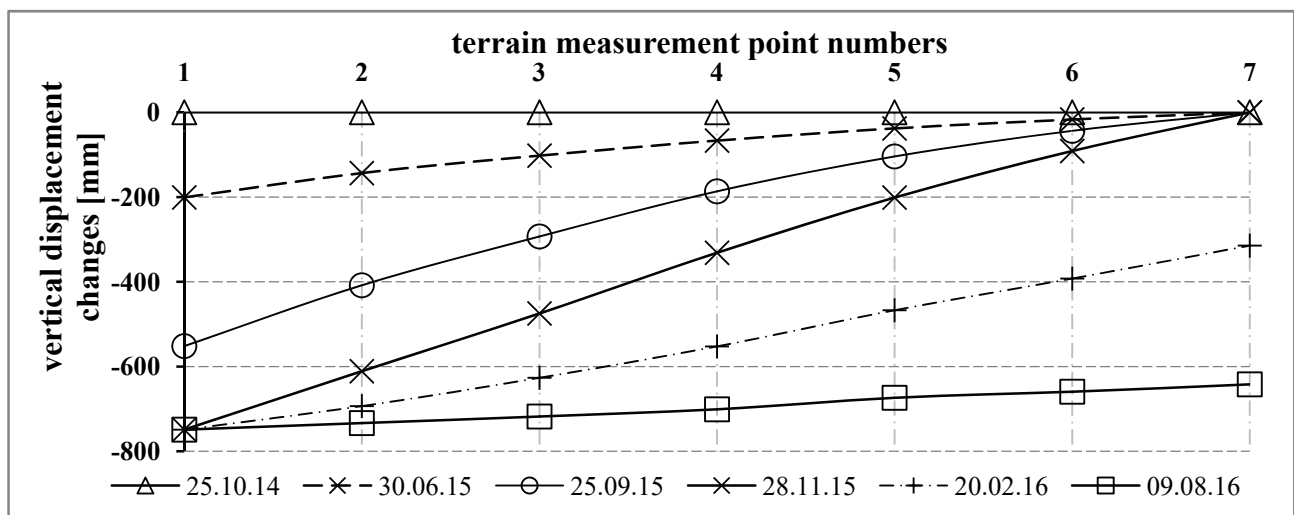

Fig. 3. Relative vertical displacements of ground measured points during revealing of subsidence

Not all of the parameters mentioned previously are significantly influential on the building structure. According to [14], the parameters considered were ground curvature K and horizontal strain ε. The displacements of the measured points allowed us to describe the extreme value of the radius of convex curvature $R = 33$ km and tensile horizontal strain $\varepsilon = 0.9$ mm/m. These parameters were achieved by using of method of precision levelling for curvature and measurement of changes in the length of individual sections of the line for horizontal strain. This values were applied in further numerical calculations.

4. Basic assumption for numerical analysis

4.1. Geometry of the numerical model

The geometry of the numerical model was adopted directly from real structures (Section 3.1). The model includes the structural elements, which have an influence on the rigidity of the structure. All wooden elements, such as ceiling beams or roof structure, were omitted. The building was settled on a bench foundation. The footings were 0.8 m and 1.0 m wide and were assumed to be of the same material as the masonry located above.

The soil below and around the building was modelled based on the soil-structure interactions. The layer of the ground below the foundation had thickness of 3.0 m and the side zone of the ground block had a width of 3.0 m outside the external surface of the basement walls. The parameters of the ground for the numerical calculation were adopted as above. The numerical model of the soil-structure interaction assumed for the calculation is presented in Fig. 4.
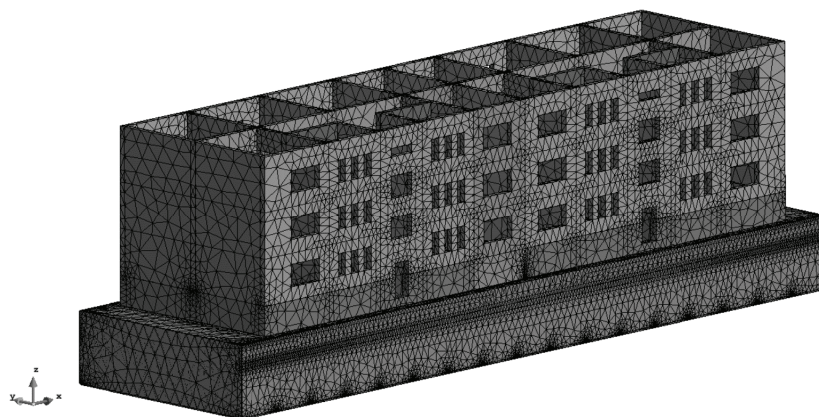

Fig. 4. 3D FEM numerical model of the soil-structure interaction system with FE mesh

4.2. Method of applying to the structure

For the most realistic representation of the object's loads, the loads were divided into two parts. The first part included typical dead and service loads. The dead load of the wall structure was implemented as a volume load but the timber ceiling, timber roof and service load of repeating floors were put on the walls on each level of the floors. The values of the volumetric loads (masonry) were assumed to be 23.0 kN/m^3 and the surface loads on the levels of the floors were between 17.0 and 64.0 kN/m^2. Those service and dead loads were applied to the structure in three proportional steps.

The other part of the loading was the ground deformation. These deformations were implemented to the block of the ground which was supported in a perpendicular direction to the bottom and side surfaces of the block. According to the measured values of the moved measured points and the theory of deformation prediction [9], the displacements caused by the radius of curvature R and horizontal strain ε were introduced into the supports of the ground block. The directions R and ε changed along the long wall of the structure. In Fig. 3, a strain of the ground can be seen, which shows the edge zone of the created subsiding basin. The measurement of the subsidence period did not recognise the concave shape of curvature K and compacting horizontal strain ε. This caused a situation when the building was loaded only by a convex part of the basin edge and horizontal strain. These deformations have been divided into two parts:

- increasing the curvature and horizontal deformation from the straight surface to the maximal bend of convex curvature ($R = +33.0$ km) and tensile horizontal strain ($\varepsilon = +0.9$ mm/m),
- reducing curvature and horizontal strain to achieve the initial state – a flat surface.

Each of the above parts were divided into three loading steps.

4.3. Basic information about numerical model

The analysis was carried out using the ATENA commercial software, made by Červenka Consulting, which used Finite Element Methods for volume as well as plane (shell) elements. The material models were defined in the software and can be chosen for particular needs, depending on the problem being solved. Two different materials were used for volume elements and one for the contact layer. All masonry structures were modelled by a defined cementitious material with a boundary surface described on the basis of the three-parameter *Willam-Warnke* model. The soil was modelled by the material model with the *Drucker-Prager* boundary surface. The interface layer, between the foundation footing and below the ground, could transmit full compression strength, zero tensile strength and 0.25 friction coefficient. All material models used the non-elastic behaviour of the

material. The basic parameters of that material are presented in Tab. 1 and a detailed description was given in [26].

Tab. 1. Basic parameters of the material model

Material	Parameters of material model				Material model type
Masonry	f_c [MPa]	f_t [MPa]	E [MPa]	v [-]	cementitious
	2.2	0.2	900	0.22	
Soil	φ [°]	c [MPa]	E [MPa]	v [-]	Drucker-Prager
	18	0.032	30	0.25	

The numerical calculations were carried out with tetrahedral FE, for volume elements, and prismatic FE, for shell elements. The whole of the numerical model was composed of about 219,000 tetrahedral elements, 2,600 prismatic elements and 69,000 nodes. The numerical model with mesh is presented in Fig. 4.

5. The results of the numerical analyses

The results of the numerical analyses were presented in the form of stress maps in the longitudinal walls. Due to the nature of terrain deformation strain, an increase in σ stress has been found. The following maps show vertical σ_{zz}, horizontal σ_{xx}, maximal σ_{max} and minimal (principal) stresses σ_{min}. Vertical stresses σ_{zz} do not change significantly (Fig. 5 and 6).

In order to present the actual behaviour of the object under the influence of ground deformation, the loads were applied in the subsequent calculation steps. The first three calculation steps included all the predicted loads in accordance with the standards in force, these were dead and service loads. In twenty consecutive steps, deformations corresponding to the passage of the entire edge of the mining basin were applied. Thus, in the fifth step, the extreme convex curvature was achieved, and in the fifteenth one the extreme concave curve. The other characteristic values of the basin edge are as followed the start of the terrain deformation process, the transition from the convex to the concave part, and then the return to the state before the ground deformation. Those values are achieved in the calculation steps 0th, 10th, and 20th. Due to the greatest influence of the ground deformation corresponding to the convex curvature only half of the calculation results are shown (calculation steps 0th to 10th). To get the full results the three initial steps were taken into account (step 1st to 3rd), so that corresponds to the following calculation steps:

- 3rd calculation step – all dead and service loads,
- 8th calculation step – the extreme value of convex curvature K and tensile horizontal strain ε,
- 13th calculation step – decreasing of the K and ε values to the initial state (3rd step).
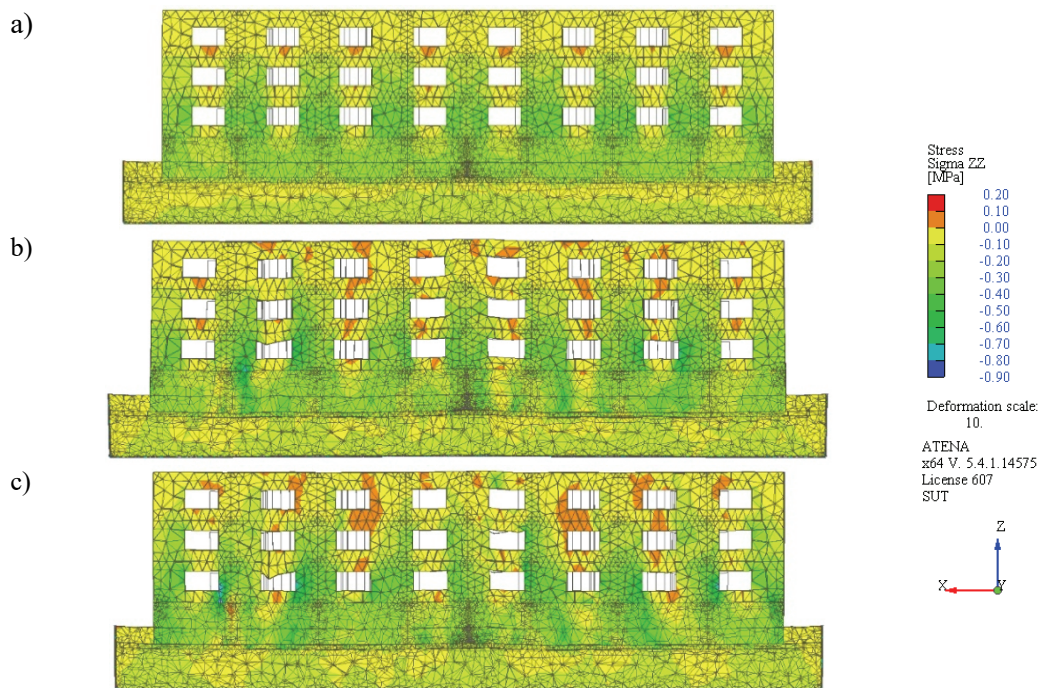
Fig. 5. Vertical stresses σ_{zz} for longitudinal (external) wall A for: a) 3rd step of calculation, b) 8th step of calculation, c) 13th step of calculation
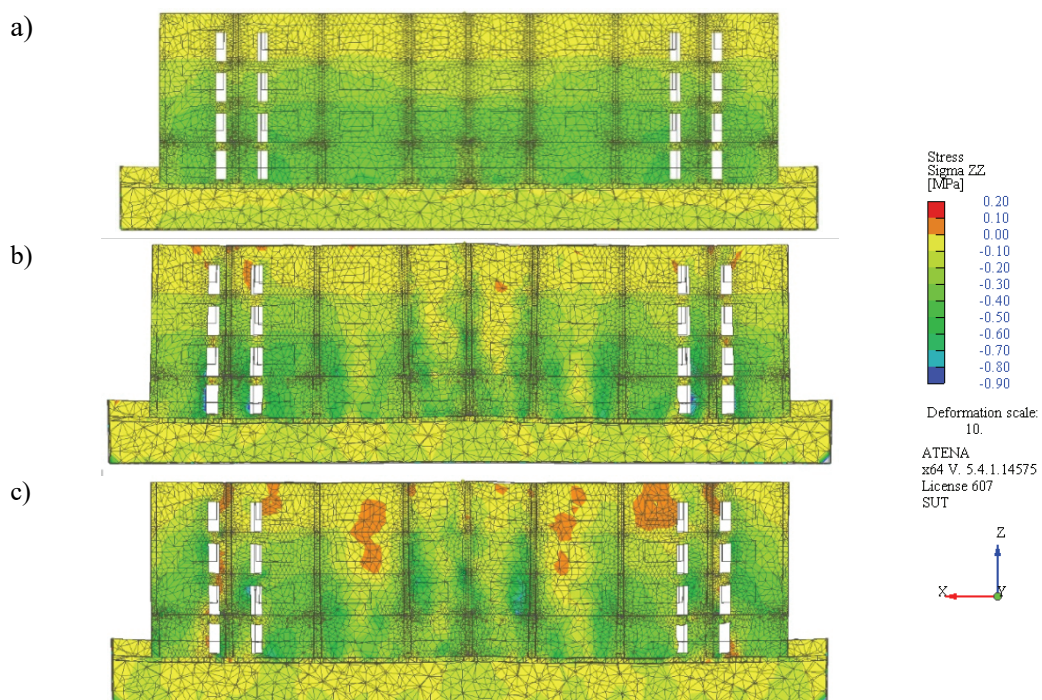

Fig. 6. Vertical stresses σ_{zz} for longitudinal (internal) wall B for: a) 3rd step of calculation, b) 8th step of calculation, c) 13th step of calculation

The extremal stresses do not exceed the compressive stress (–0.8 MPa) and tensile stress (0.1 MPa), which are below the strength of the material (Section 3.1 and Tab. 1).

While the ground deformations are revealing, the horizontal stresses are changed. That were showed for external (A axis) Fig. 7 and internal longitudinal wall (B axis) on the Fig. 8.
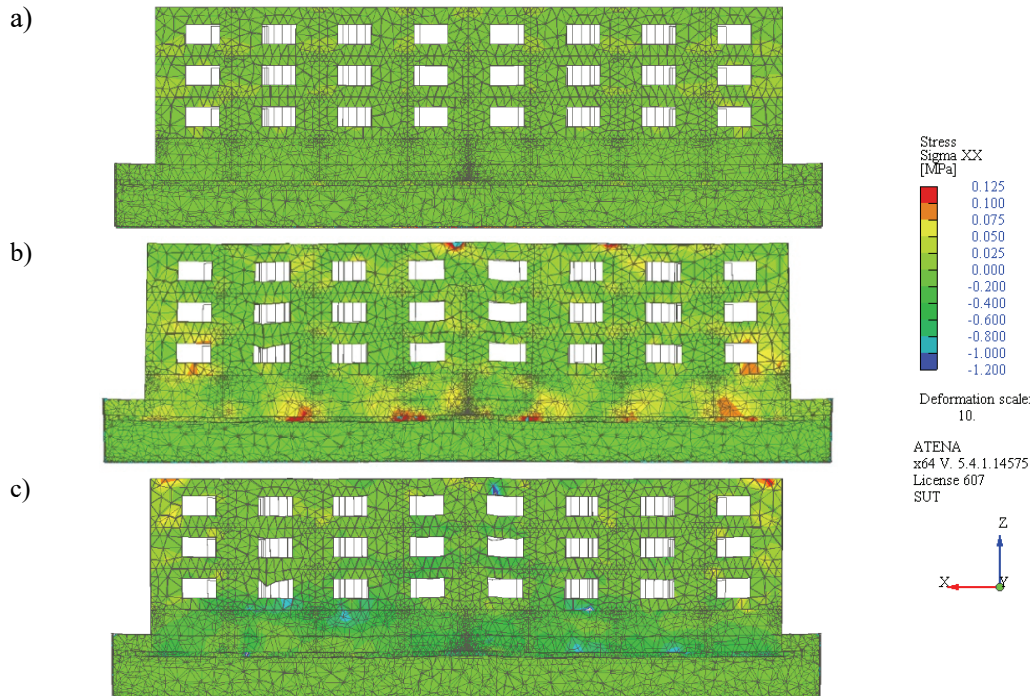

Fig. 7. Horizontal stresses σ_{xx} for longitudinal (external) wall A for: a) 3rd step of calculation, b) 8th step of calculation, c) 13th step of calculation
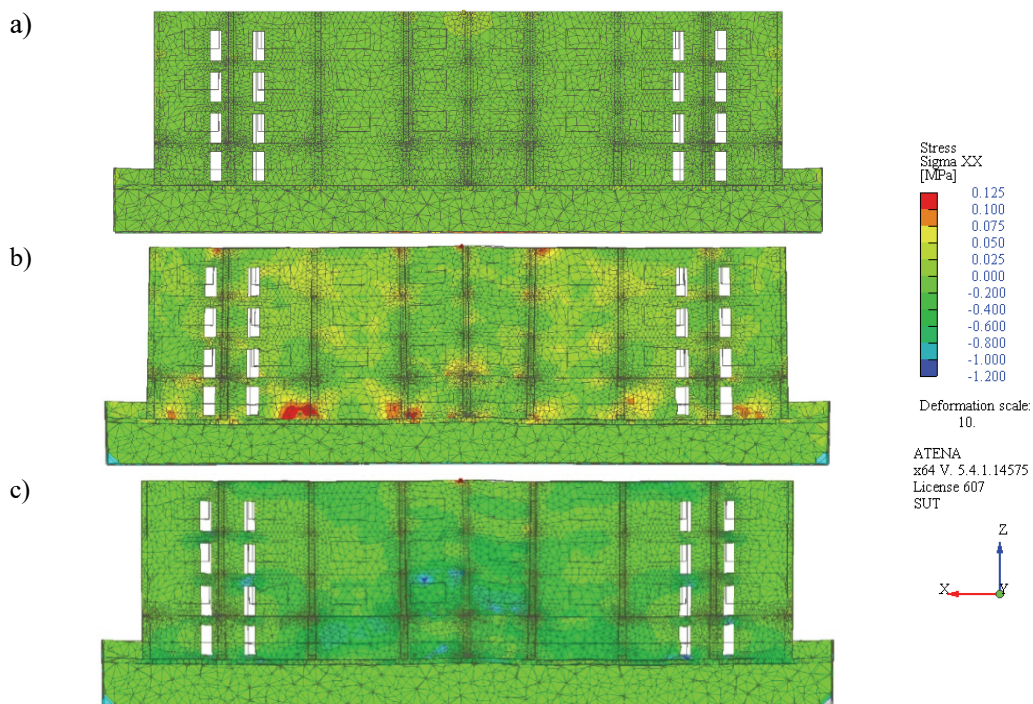

Fig. 8. Horizontal stresses σ_{xx} for longitudinal (internal) wall B for: a) 3rd step of calculation, b) 8th step of calculation, c) 13th step of calculation

The horizontal stresses σ_{xx} presented in Fig. 7 and 8 show visible changes. The increased effects of stress is caused by the horizontal strain of soil and is focused in the lower part of the walls (Fig. 7b, and 8b). The curvature influence is not so significant but some concentration of stress is visible in the upper part of the window zone of the walls. The values of stresses σ_{xx} do not yet reach the level of tensile strength f_t, but principal stresses σ_{max} exceed that value, as shown in Fig. 9. The cracks in the walls presented in Fig. 9 are located near openings in the middle part of the structure.
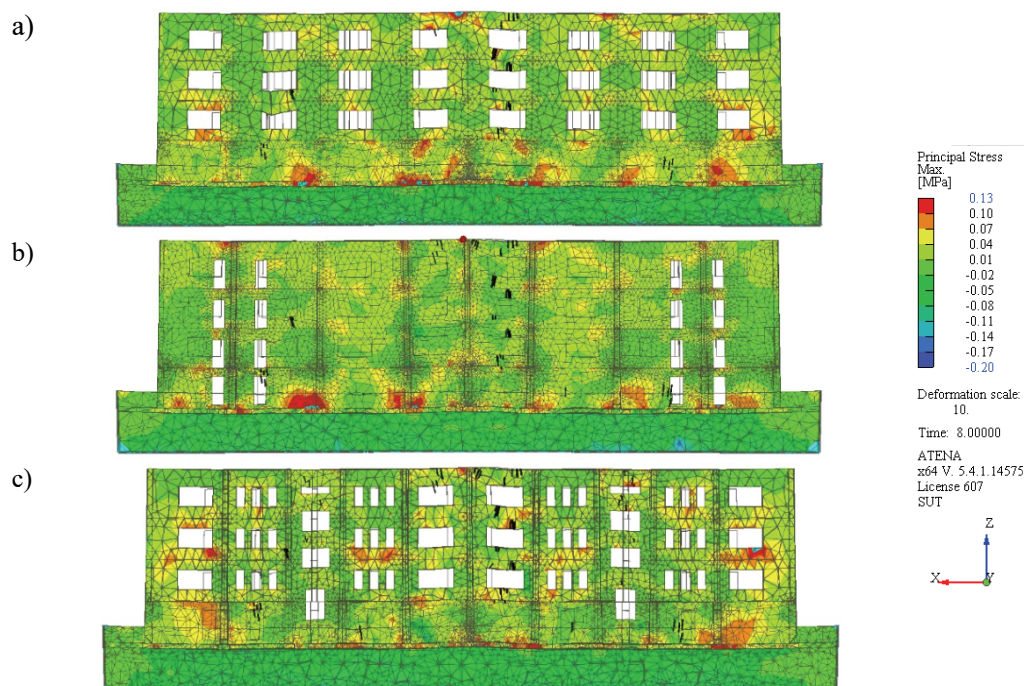

Fig. 9. Principal stresses σ_{max} for longitudinal walls and cracks for the 8th step of calculation: a) longitudinal wall A, b) longitudinal wall B, c) longitudinal wall C

In the 8th step of the numerical calculation, there is a mix of the convex soil curvature and tensile horizontal strain. The related stresses in the walls are not obviously clear and the concentration of stress is visible in the upper to middle part of the element (caused by curvature) as well as the lower part (caused by horizontal strain). The most focused stresses are placed near the openings of the structures, which decreases the bearing capacity and rigidity of the wall. This is a potential region for cracking to develop but the maps presented show maximal stresses σ_{max} (0.13 MPa) below the tensile strength f_t of the masonry (0.2 MPa).

The stresses below the foundation are presented in Fig. 10. Maximal stresses σ_{max} (Fig. 10a) occurred outside the foundation plan and reached values up to 0.1; this is potentially due to the elastic behaviour of the soil, caused by tensile loading. Minimal stresses σ_{min} (Fig. 10b) reached values of approximately –0.2 MPa under the foundation and do not exceed the elastic behaviour of soil.
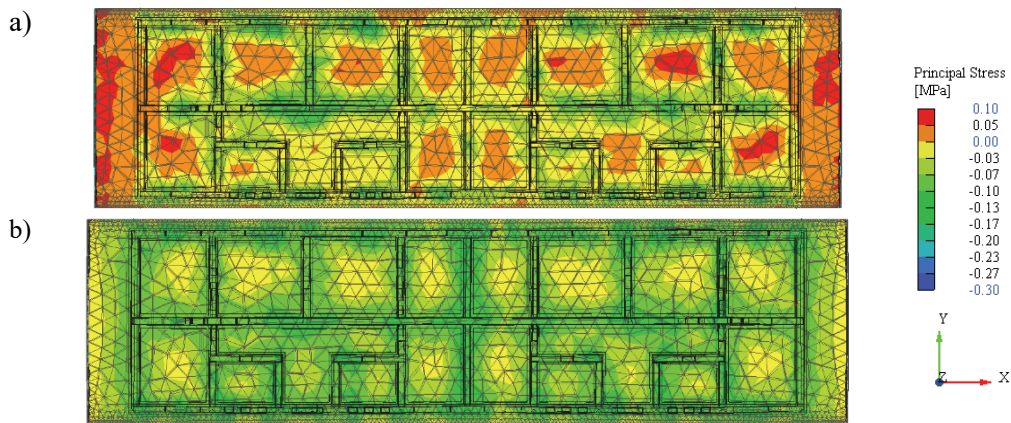
a)

b)

Fig. 10. Principal stresses below foundation in 8th calculation step: a) maximal stress σ_{max}, b) minimal stresses σ_{min}

6. Summary and conclusion

The main purpose of the analysis was to determine the behaviour of the building under the influence of ground deformation. The numerical analyses were carried out for the soil-structure interaction system and the deformations were introduced into the system by soil block support displacement. The block of soil was loaded by soil displacement, corresponding to the convex curvature of the area (with a radius of 33.0 km) and horizontal strain of 0.9 mm/m. The deformations were applied to the bottom and the side surface of the block. The deformation values were calculated by means of geodetic measurement and the shapes of the deformations were described by *Knothe* (1953). The modelled structures only consisted of the bearing element of the walls and the foundations, the timber elements of the ceiling beam and roof were omitted. It was assumed that the whole of the computational model of the building would be modelled as masonry elements with isotropic properties, on the basis of the concrete ones. The material parameters of the soil were assumed to be clay. The material parameters used in the numerical calculations are presented in Tab. 1.

The results of the computational analysis indicate a significant increase in normal horizontal stress σ_{xx} in the wall elements, located parallel to the direction of mining exploitation. Extreme values occur in the upper section of the wall (caused by the curvature of the soil) and the bottom section (caused by the horizontal deformation of the soil). The magnitude of these stresses in the calculation steps, both before the occurrence of deformations and in the case of the largest impact of the substrate deformation, is shown in Fig. 7 and 8. A decisive factor for the occurrence of wall cracking is the tensile principal stress σ_{max}, which is presented in Fig. 9 for an 8th step calculation with the shortest radius of convex curvature and tensile horizontal deformation. The concentration

of these stresses also occurs in the places as the horizontal stresses σ_{xx}. The highest stress σ_{max} concentrations occur where the wall stiffness decreases, i.e. in the corners of window and door openings. Stress levels do not exceed the uniaxial tensile strength f_t but the complex stress state in the elements reveals the possibility of cracking (Fig. 9). The results of the analysis coincide with the observed damage to the actual building studied. On this basis, it can be concluded that the assumptions adopted in the analysis of the soil-structure interaction system correctly reflect reality.

Acknowledgements:

References

[1] Ochrona powierzchni przed szkodami górniczymi, Group work, Publishing House Śląsk; 1980.

[2] J. Rusek, L. Słowik, K. Firek, M. Pitas, "Determining the Dynamic Resistance of Existing Steel Industrial Hall Structures for Areas with Different Seismic Activity". Archives of Civil Engineering LXVI(4): 2020; pp. 525–542; https://doi.org/10.24425/ace.2020.135235.

[3] J. Rusek, W. Kocot, "Proposed Assessment of Dynamic Resistance of the Existing Industrial Portal Frame Building Structures to the Impact of Mining Tremors". 2017 IOP Conference Series Materials Science and Engineering; 245(3):032020; https://doi.org/10.1088/1757-899X/245/3/032020.

[4] J. Rusek, K. Tajduś, K. Firek, A. Jędrzejczyk, "Bayesian networks and Support Vector Classifier in damage risk assessment of RC prefabricated building structures in mining areas". 2020 5th International Conference on Smart and Sustainable Technologies (SpliTech); DOI: 10.23919/SpliTech49282.2020.9243718

[5] Y. Jiang, R. Misa, K. Tajduś, A. Sroka, Y. Jiang, "A new prediction model of surface subsidence with Cauchy distribution in the coal mine of thick topsoil condition". Archives of Mining Sciences 65(1): 2020; pp. 147–158; https://doi.org/10.24425/ams.2020.132712.

[6] A. Sroka, S. Knothe, K. Tajduś, R Misa., "Point Movement Trace Vs. The Range Of Mining Exploitation Effects In The Rock Mass". Archives of Mining Sciences, Vol. 60 (2015), No 4, pp. 921–929; https://doi.org/10.1515/amsc-2015-0060

[7] K. Tajduś, "Analysis of horizontal displacement distribution caused by single advancing longwall panel excavation". Journal of Rock Mechanics and Geotechnical Engineering 1(4) 2015; https://doi.org/10.1016/j.jrmge.2015.03.012.

[8] R. Bals, "Beitrag zur Frage der Vorausberechnung bergbaulicher Senkungen. Mitteilungen aus dem Markscheidewese". Verlag Konrad Witter. Stuttgart; 1931/32.

[9] Knothe S., „Równanie profilu ostatecznie wykształconej niecki osiadania", Archiwum Górnictwa i Hutnictwa, 1953, t.1, z.1.

[10] W. Ehrhard, A. Sauer, "Die Vorausberechnung von Senkung, Schieflage und Krummung uber dem Abbau in flacher Lagerung". Bergbau-Wissenschaften, 1961.

[11] K. Tajduś, "Numerical Simulation of Underground Mining Exploitation Influence Upon Terrain Surface". Archives of Mining Sciences 58(3) 2013; https://doi.org/10.2478/amsc-2013-0042.

[12] M. Cała, J. Flisiak, A. Tajduś, „Wpływ niepodsadzkowych wyrobisk przyszybowych na deformacje powierzchni. Człowiek i środowisko wobec procesu restrukturyzacji górnictwa węgla kamiennego". Biblioteka Szkoły eksploatacji Podziemnej, 2001, nr 6.

[13] K. Tajduś, S. Knothe, A. Sroka, R. Misa, "Underground exploitations inside safety pillar shafts when considering the effective use of a coal deposit". Gospodarka Surowcami Mineralnymi 31(3): 2015; pp. 93–110; https://doi.org/10.1515/gospo-2015-0027.

[14] Z. Budzianowski, „Działanie wygiętego podłoża na sztywną budowlę znajdującą się w obszarze eksploatacji górniczej". Inżynieria i Budownictwo, 1964, nr 6 i 7.

[15] O. Deck, M. Al Heib, F. Homand, "Taking the soil–structure interaction into account in assessing the loading of a structure in a mining subsidence area". Engineering Structures 2003; 25, pp. 435–448; https://doi.org/10.1016/S0141-0296(02)00184-0

[16] A. Saeidi, O. Deck, T. Verdel, "Development of building vulnerability functions in subsidence regions from empirical methods". Engineering Structures 2009; 31 (10), pp. 2275–2286; https://doi.org/10.1016/j.engstruct.2009.04.010

[17] J. Kwiatek, "Protection of construction objects in mining areas". Publishing House of Central Mining Institute, Katowice, (in Polish) 1997; p. 726.

[18] J. Kwiatek, "Construction facilities on mining areas". Wyd. GiG Katowice (in Polish), 2007; p. 266.

[19] L. Szojda, "Numerical analysis of the influence of non-continuous ground displacement on masonry structure". Silesian University of Technology Publishing House, Gliwice, Monography (in Polish), p. 194; 2009.

[20] D. Mrozek, M. Mrozek, J. Fedorowicz, "The protection of masonry buildings in a mining area". Procedia Engineering 193 International Conference on Analytical Models and New Concepts in Concrete and Masonry Structures AMCM'2017, pp.184–191; https://doi.org/10.1016/j.proeng.2017.06.202

[21] R. Misa, K. Tajduś, A. Sroka, "Impact of geotechnical barrier modelled in the vicinity of a building structures located in mining area". Archives of Mining Sciences 2018; no 4, vol. 63 Kraków, pp. 919–933; https://doi.org/10.24425/ams.2018.124984

[22] A. Sroka, R. Misa, K. Tajduś, M. Dudek, "Analytical design of selected geotechnical solutions which protect civil structures from the effects of underground mining". https://doi.org/10.1016/j.jsm.2018.10.002

[23] L. Szojda, Ł. Kapusta, "Evaluation of the elastic model of a building on a curved mining ground based on the result of geodetic monitoring". Archives of Mining Sciences 65(2): 2020; pp. 213–224, https://doi.org/10.24425/ams.2020.133188

[24] L. Szojda, G. Wandzik, "Discontinuous terrain deformation - forecasting and consequences of their occurrence for building structures". 29th International Conference on Structural Failures, 2019, art. no. 03010 pp. 1–12, https://doi.org/10.1051/matecconf/201928403010

[25] L. Szojda, „Analiza numeryczna zmian naprężeń w konstrukcji ściany wywołanych nieciągłymi deformacjami podłoża górniczego". Czasopismo Inżynierii Lądowej, Środowiska i Architektury, 2017 t. 34 z. 64, nr 3/I, p. 511–522, https://doi.org/10.7862/rb.2017.142

[26] V. Červenka, L. Jendele, J. Červenka, "ATENA Program documentation". Part 1, Theory, Prague, 2016, p. 330.

Analiza numeryczna wpływu deformacji podłoża górniczego na konstrukcję murowanego budynku mieszkalnego

Słowa kluczowe: konstrukcja murowa, analiza numeryczna, górnicze osiadania terenu, krzywizna terenu, poziome odkształcenia terenu

Streszczenie:

Starzejąca się struktura zabudowy miast w rejonach eksploatacji górniczej wpływa znacznie na zwiększenie kosztów naprawy uszkodzeń obiektów powierzchni. Prognozowanie zachowania się budynków pod wpływem deformacji podłoża w przypadku, gdy nie są one do tego przystosowane staje się bardzo istotne z punktu widzenia bezpieczeństwa tych konstrukcji. Stało się to przyczyną przedstawienia przykładu analizy numerycznej typowego budynku mieszkalnego obszaru Górnego Śląska, który powstał w początkach XX wieku i nie był przystosowany do przeniesienia górniczych deformacji terenu. W celu dokładnego odwzorowania zachowania się obiektu pod wpływem deformującego się podłoża przeprowadzono analizę układu budowla – podłoże, w tym przypadku górnicze. Autorzy, posiadając wiedzę kiedy oraz w jakim obszarze będą ujawniały się osiadania na skutek wyeksploatowanej ściany, zastabilizowali układ punktów pomiarowych w najbliższym sąsiedztwie budynku oraz na ścianach podłużnych budynku. Wyniki pomiarów poziomych i pionowych przemieszczeń posłużył do ich wprowadzenia w modelu obliczeniowym. Zgodnie z teoriami prognozowania górniczych deformacji terenu typu ciągłego największy wpływ na budynki mają poziome deformacje podłoża   i krzywizna terenu K. Charakterystyki przebiegów tych zmiennych przyjęto wg teorii *Knothego*. Wpływy te należy rozważać jako dodatkowe obciążenia budynku, ale nie należy ich przykładać bezpośrednio do konstrukcji, lecz jako odkształcenia podłoża. Z tego powodu obliczenia numeryczne objęły budynek oraz bryłę podłoża aby uwzględnić efekt współpracy budowla–podłoże. Konstrukcja budynku była murowana z drewnianymi elementami stropów i dachu, które ze względu na znikomy wpływ sztywność pominięto w obliczeniach numerycznych. Bryła podłoża została tak dobrana, że obejmowała warstwę o grubości 3,0 m poniżej fundamentów oraz 3,0m na zewnątrz rzutu budynku.

Pionowe i poziome powierzchnie bryły gruntu zostały podparte przegubowo w kierunku prostopadłym do ich powierzchni. Analizę numeryczną wykonano przy użyciu pakietu programów Atena i dla każdego z materiałów układu wprowadzono odpowiedni model materiałowy – dla gruntu model *Druckera-Pragera*, a dla elementów murowych model sprężysto-plastyczny opisany w pakiecie jako '*cemetitous*', który wykorzystuje powierzchnię graniczną przedstawioną przez *Willama-Warnke*. Obciążenia konstrukcji podzielono na kilka etapów. W pierwszym etapie przyłożono obciążenia stałe i użytkowe budynku (3 kroki obliczeniowe), a w drugim deformacje podłoża. Odwzorowano przejście wypukłej części krawędzi niecki górniczej, które podzielono na 10 kroków obciążeniowych. Powstania maksymalnej krzywizny wypukłej $K+$ i odkształcenia podłoża $\varepsilon+$ osiągnięto w 8 kroku obciążeniowym, a powrót do stanu początkowego w 13. Wyniki analiz przedstawiono w postaci barwnych map naprężeń. Najistotniejsze wyniki to wielkość głównych naprężeń rozciągających, w zależności od których mogą powstawać zarysowania konstrukcji po przekroczeniu wytrzymałości na rozciąganie. Na mapach wyraźne ich koncentracje pojawiają się w górnej części ścian konstrukcji oraz w narożach otworów okiennych i drzwiowych. Jest to zgodne z obserwacjami na obiektach, które zostały poddane takim deformacjom. Przedstawiony sposób może zostać wykorzystany w szczegółowym podejściu do analizy zagrożonych obiektów budowlanych.